Author response – Editor

We thank the editor for his important feedbacks. Our author responses are shown in blue.

1) Negative emissions in your results: in your response (Figure 3) and the supplement (Figure S5), scatter plots of posterior emissions show both negative emissions on many grid cells over many weekly time steps. It also seems to show a small number of very high emissions values in some cases over a small number of grid cells over a small number of weekly time steps. You have cited (Zheng et al., 2026 ACP) which demonstrates that physically unrealistic negative emissions arise from the nonlinear propagation of noise and should be filtered out. It is also consistent with the small number of very high emissions points observed. Please clarify:

- Are the values shown in Figure 3 after applying the noise-threshold filter described in Zheng et al., 2026?
- If yes, why do negative values persist?
- If no, please apply the filter and show the filtered results. Alternatively, explicitly state that you have not applied such filtering and discuss the implications for your emission estimates.

Some negative values are already present in the prior dataset, mostly located in two blobs, in the north-western part and in the northern part of the domain (Figure 1, first map). These pixels (6.4% of the pixels) correspond to negative fluxes in the ocean climatology input emissions and have very low absolute magnitude. Other areas with soil sinks have negative prior values, also with low magnitude. They do not significantly contribute to total emissions or European budgets.

These negative emissions can also be seen in the posterior in the inversions. However, as you mention, there are additional negative emissions in the results. The emissions are assumed to be normally distributed, thus the optimization of the control vector allows negative values.

For the SRON, BLENDED, WFMD and Surface inversions, there are respectively 6.6%, 6.4%, 8.2% and 7.1% of the posterior control vector values that are negative (one control vector value = emissions of a 0.5°x0.5° pixel for one week). The additional negative emissions are located in Italy, Central Europe and Northern Africa (Figure 1).

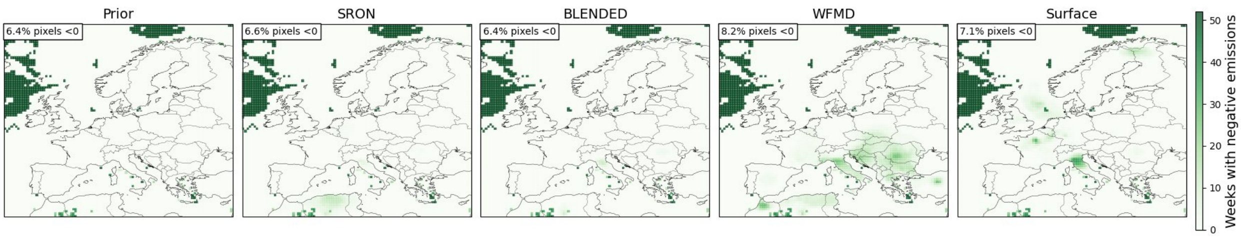

Figure 1: Number of weeks with negative emissions, for all 0.5° pixel, in the prior and posteriors.

As you recommend, we applied the noise-threshold filter described in Zheng et al. (2026). As our inversions are Bayesian inversions (a difference with the cited work), the values that are filtered out in the posterior emissions are replaced by the corresponding prior value. Also, negative emissions corresponding to negative prior emissions (reported natural sinks) are not filtered out. Most strong negative values are indeed filtered out (Figure 2), especially those in the areas mentioned in the previous paragraph (Figure 3). The rest of the distribution is similar, for the four inversions.

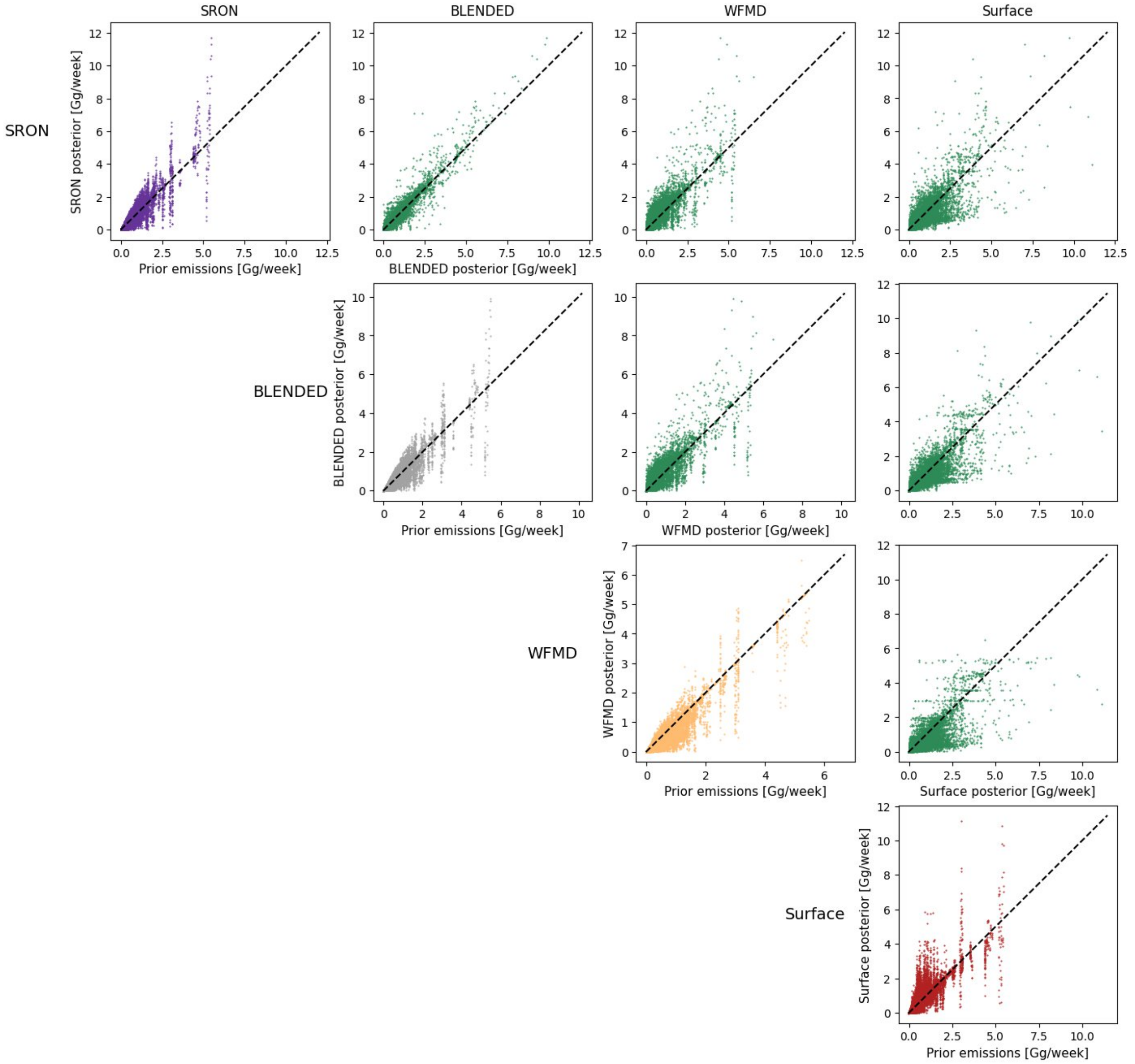

Figure 2: Same as Figure 3 of the previous response, but after applying the noise-threshold filter. The diagonal plots show scatter plots of posterior against prior emissions. The non-diagonal plots show a comparison of the posterior emissions. The dashed line is the 1:1 line.

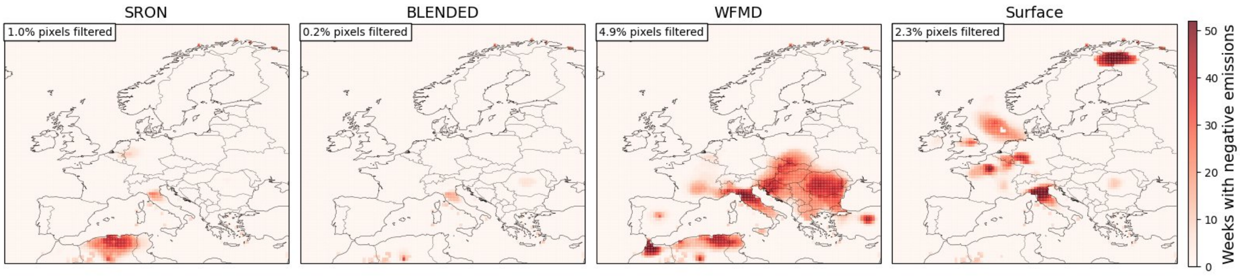

Figure 3: Number of weeks with negative values, for each 0.5°x0.5° pixel, in the prior and the posterior emissions.

The impact of the filter on the CH_4 European emission estimates in 2019 is shown in Table 1. As negative values are removed and replaced with the corresponding prior values, the budget estimates are increased in all the inversions, and are closer to the prior total (except for SRON, for which the estimate is slightly higher than the prior). In particular, the strong negative increments of WFMD in Italy and Central Europe are reduced, leading to a higher total of emissions. In practice, applying this filter gives more confidence to the prior.

When applying the filter, the conclusions of the study remain valid: building country-scale budgets with the emissions estimated from regional inversions of TROPOMI XCH_4 data should be done with caution, as the estimated emissions show significant relative differences across products, in the total and country budgets as well as in the spatial and temporal distributions of emissions.

Inversion	**Posterior, without the filter (Tg/yr)**	**Posterior, with the filter (Tg/yr)**
SRON	25.7	26.0
BLENDED	25.0	25.2
WFMD	16.9	21.2
Surface	23.0	25.1

Table 1: European CH_4 budget for 2019, without and with the noise-threshold filter described in Zheng et al. (2026). The total of prior emissions is 25.2 Tg/yr.

Given that the conclusions are not changed, and to remain in the framework of Bayesian inversions, we choose not to apply the filter. Indeed, truncating gaussian distributions in this framework require accurate statistical sampling of the new estimate of the analysis after truncating (Lauvernet et al., 2009), going beyond the variational inversions performed in this study. Though, work has to be done to treat the negative values: either by adapting rigorously the noise-threshold filter to the framework of Bayesian inversions, or by using log-normal distributions for the emissions to ensure positive fluxes (while optimizing sinks separately). The latter and more direct approach, mentioned in Zheng et al. (2026), has been used in recent works (Bergamaschi et al., 2022 ; Hancock et al., 2025). To mention this issue, a discussion on negative emissions has been added to the text (Section 3.3).

2) Spatial scale inconsistency - “not point sources” but still attributing to basins
You state that your inversion is designed for basin scale and large sources, not point sources, and that you cannot validate at the native TROPOMI resolution. However, your model grid is 0.5° (approx. 50 km). At this scale, a single grid cell in regions like the Upper Silesian Coal Basin in your region, or many other coal basins around the world (such as the Changzhi Basin) contains a mixture of coal mines, industrial facilities, and natural areas. Therefore, claiming that your results are “basin scale” does not relieve you from the need to demonstrate that your emissions are physically plausible at the grid cell level, especially when you compare to independent local studies (e.g., Tu et al., 2022). Remember that TROPOMI spatial scale (5.5km x 7km approx.) is still not point source scale, yet is far finer than the chosen model scale. Please add a clear statement in the manuscript (and, if necessary, in the response) that:

- Your inversion cannot attribute emissions to specific point sources or to individual source sectors (e.g., coal vs. agriculture) within a 0.5° grid cell.
- Any comparison with local studies (e.g., Tu et al., 2022) should be interpreted with caution because of the scale mismatch.

The statements have been added to the manuscript (Section 3.3 and Conclusion). We confirm that the inversion can not disentangle source sectors within a 0.5° grid cell, as well as individual point sources as mentioned in the previous response. The expression « basin scale » may have been poorly used in our response: we claim that it is not relevant to compare directly the emissions at the grid cell level, this is why we compare national budgets and average maps in the article.

The comparisons with local studies have been made to address the questions of a reviewer: we definitely agree that they should be interpreted with caution. We emphasize this point in the clarifications that have been added to the text.

3) Day-by day, grid by grid validation: a reviewer requested a scatterplot of modeled vs. observed XCH4. Please provide a representative example (e.g., for a few weeks in a key region) showing the correlation between observed and simulated XCH4 after the inversion, aggregated to your 0.5° model grid. This will help readers assess whether the inversion is fitting the data in a physically reasonable way.

> Additionally, for a small subset of grid cells (e.g., 5-10 cells covering different land uses), please report the standard deviation (or 10th-90th percentile range) of the native TROPOMI pixels that contribute to each 0.5° average. This will indicate whether the averaging hides significant spatial heterogeneity that could bias the inversion.

The scatter plots of observed and simulated XCH4 before and after the inversion are shown in Figure 4 for all observations, aggregated to the 0.5° model grid. The fit between modeled and observed XCH4 is improved, as shows the increase of the correlation coefficient R^2 for all inversions . When looking at a specific region (2°-10° longitude, 48°-54° latitude, covering Germany, the Netherlands, Belgium, Luxembourg and eastern France) where the initial fit is poor, the fit of the data after the inversion seems physically reasonable, with a substantial increase of R^2 (Figure 5). Figure 4 has been added to the supplementary material, complementing the maps of Figure 9 in the manuscript.

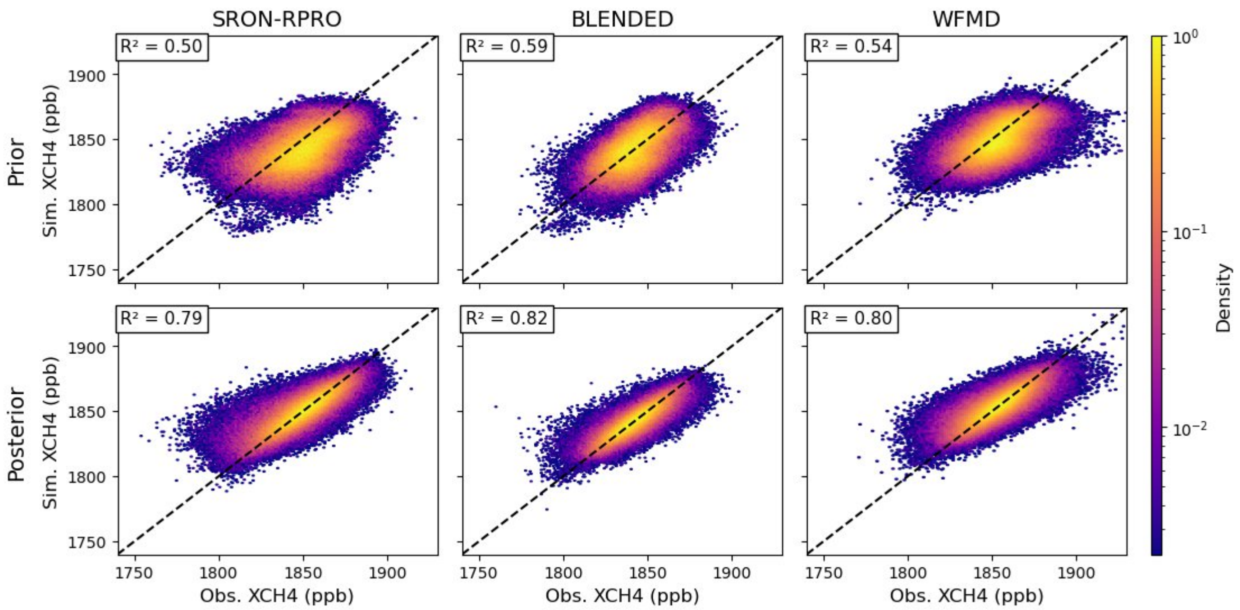

Figure 4: Hexagonal binning plots of the modeled and observed XCH_4 for the satellite inversions, using prior emissions (first row) and posterior emissions (second row). R^2 is the correlation coefficient. The dashed black line is the 1:1 line.

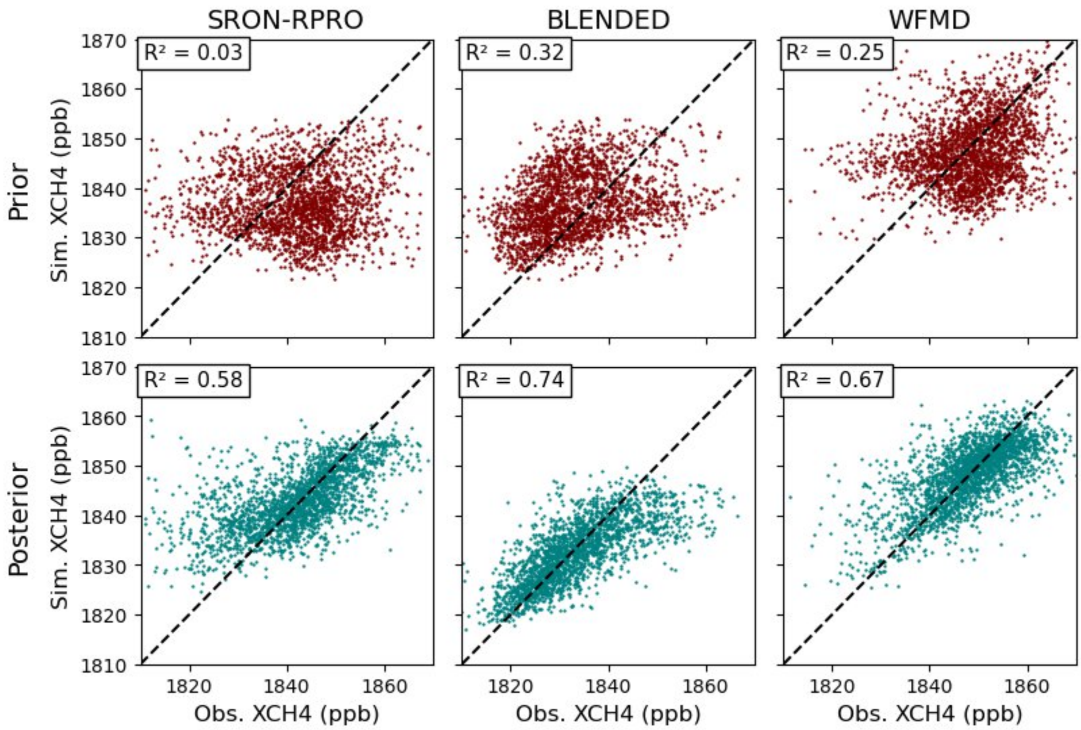

Figure 5: Scatter plots of the modeled and observed XCH_4 for the satellite inversions, using prior emissions (first row) and posterior emissions (second row), in the region covering 2°-10° longitude and 48°-54° latitude.

Regarding the spatial heterogeneity, the standard deviation of TROPOMI XCH4 in the 0.5°x0.5° pixel is shown for a few pixels in Figure 6. The selected pixels are shown on the map, and for all products the deviation are in the range 10 to 25 ppb, which is of the order of magnitude of the observation errors. When considering all pixels, the deviations mostly range between 0 and 25 ppb, with a maximum of pixels below (SRON, BLENDED) or around (WFMD) 10 ppb (Figure 7).

In the inversion, observations are assimilated individually: the inversion is not directly affected by aggregation effects, though the system has to fit multiple observation values that are in the same model spatio-temporal grid cell. This is an indirect effect of the spatial heterogeneity. Accounting for this heterogeneity could be done through the calculation of the aggregated observation error if super-observations were used (Chen et al., 2023), which is not the case in our study.

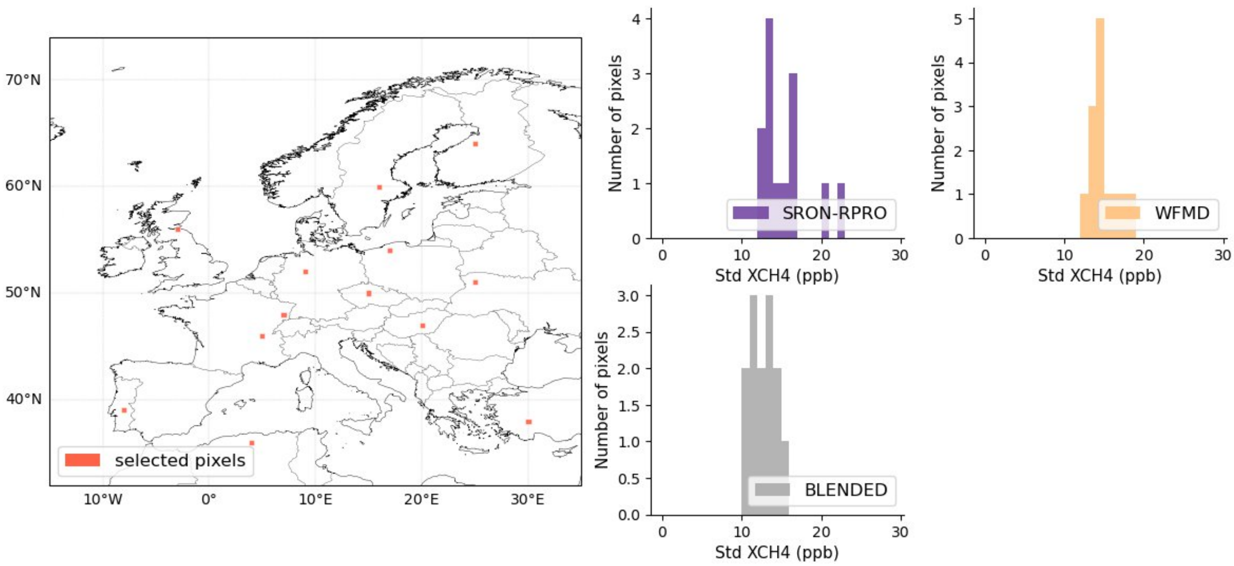

Figure 6: Standard deviations of the XCH4 observations contributing to the 0.5° averages, for all TROPOMI products and for the selected pixels pictured on the map.

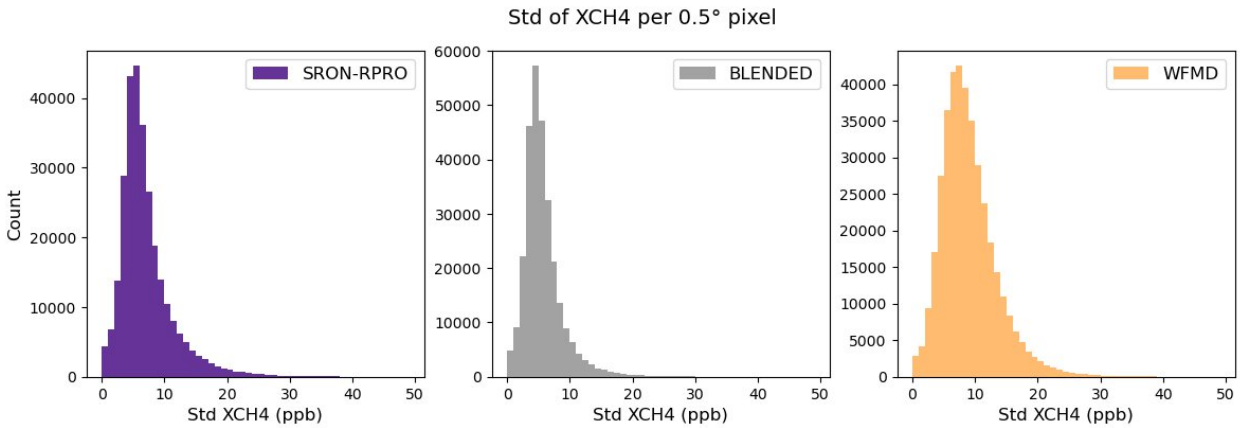

Figure 7: Distributions of the standard deviations of the XCH4 observations contributing to the 0.5° averages, for all TROPOMI products and all pixels.

References:

Bergamaschi, P., Segers, A., Brunner, D., Haussaire, J.-M., Henne, S., Ramonet, M., Arnold, T., Biermann, T., Chen, H., Conil, S., Delmotte, M., Forster, G., Frumau, A., Kubistin, D., Lan, X., Leuenberger, M., Lindauer, M., Lopez, M., Manca, G., Müller-Williams, J., O'Doherty, S., Scheeren, B., Steinbacher, M., Trisolino, P., Vítková, G., and Yver Kwok, C.: High-resolution inverse modelling of European CH4 emissions using the novel FLEXPART-COSMO TM5 4DVAR inverse modelling system, Atmos. Chem. Phys., 22, 13243–13268, https://doi.org/10.5194/acp-22-13243-2022, 2022.

Chen, Z., Jacob, D. J., Gautam, R., Omara, M., Stavins, R. N., Stowe, R. C., Nesser, H., Sulprizio, M. P., Lorente, A., Varon, D. J., Lu, X., Shen, L., Qu, Z., Pendergrass, D. C., and Hancock, S.: Satellite quantification of methane emissions and oil–gas methane intensities from individual countries in the Middle East and North Africa: implications for climate action, Atmos. Chem. Phys., 23, 5945–5967, https://doi.org/10.5194/acp-23-5945-2023, 2023.

Hancock, S. E., Jacob, D. J., Chen, Z., Nesser, H., Davitt, A., Varon, D. J., Sulprizio, M. P., Balasus, N., Estrada, L. A., Cazorla, M., Dawidowski, L., Diez, S., East, J. D., Penn, E., Randles, C. A., Worden, J., Aben, I., Parker, R. J., and Maasakkers, J. D.: Satellite quantification of methane emissions from South American countries: a high-resolution inversion of TROPOMI and GOSAT observations, Atmos. Chem. Phys., 25, 797–817, https://doi.org/10.5194/acp-25-797-2025, 2025.

Lauvernet, C., Brankart J.-M., Castruccio, F., Broquet, G., Brasseur, P., and Verron, J.: A truncated Gaussian filter for data assimilation with inequality constraints: Application to the hydrostatic stability condition in ocean models, Ocean Modelling, 27, 1–2, 1-17, https://doi.org/10.1016/j.ocemod.2008.10.007, 2009.